Supporting Information for

Nanoscale Metal-organic Frameworks for Real-Time Intracellular pH Sensing in Live Cells

Chunbai He[†], Kuangda Lu[†], and Wenbin Lin*

Department of Chemistry, University of Chicago, 929 E 57th St, Chicago, IL 60637, USA

Table of Contents

1. Materials and cell lines

All of the starting materials were purchased from Sigma-Aldrich and Fisher (USA), unless otherwise noted, and used without further purification. H460 cells (human lung cancer cells) were purchased from the American Type Culture Collection (Rockville, MD, USA) and were cultured in RPMI 1640 medium containing 10% fetal bovine serum (FBS, Gibco, Grand Island, NY, USA).

2. Synthesis of UiO nanoscale metal-organic framework (NMOF)

UiO NMOF was synthesized as described in our previous report.[1] Briefly, amino-triphenyldicarboxylic acid (amino-TPDC) as bridging ligands was mixed with dimethylformamide (DMF) solutions of $ZrCl_4$, and the mixture was kept in an 80 °C oven for 5 days. The product was collected by centrifugation and washed with DMF, triethylamine/ethanol (1:20, V/V), and ethanol.

Transmission electron microscopy (TEM, Tecnai F30 and Tecnai Spirit, FEI, USA) was utilized to confirm the morphology of UiO NMOF (Figure S1). Particle sizes of UiO NMOFs were determined by dynamic light scattering (DLS, Nano-ZS, Malvern, UK; Figure S2).

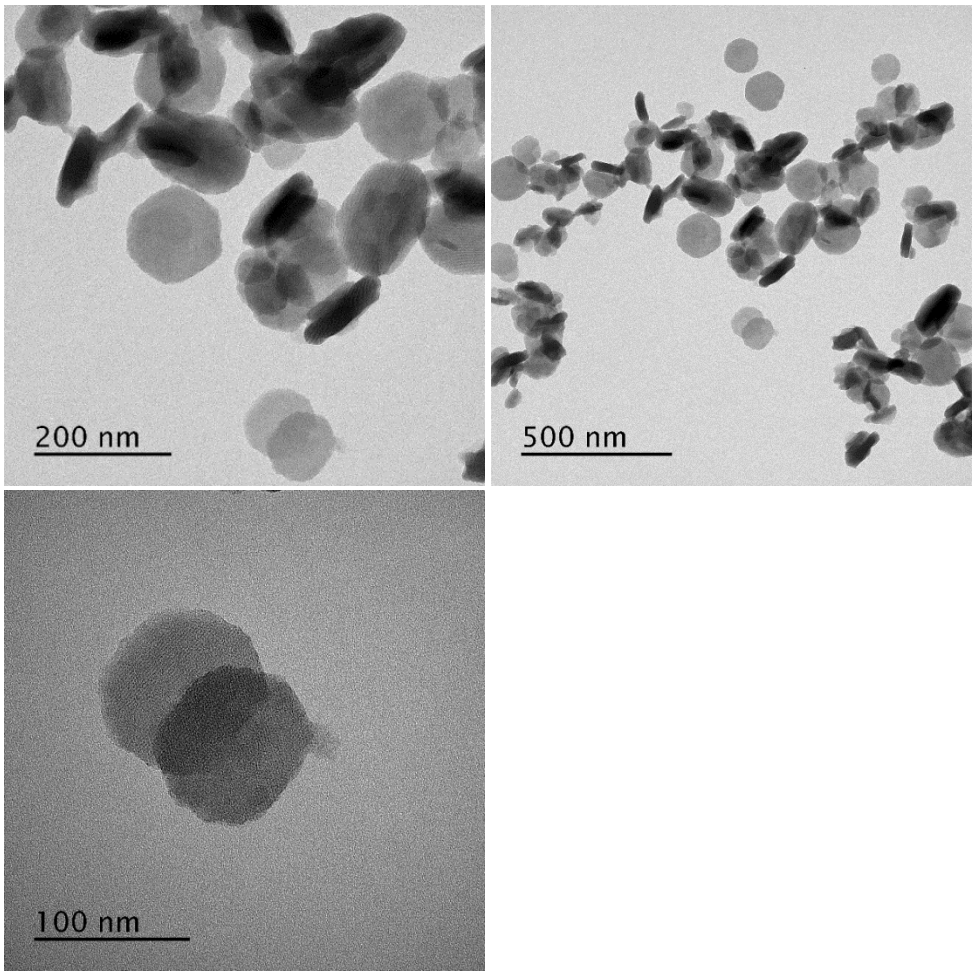

Figure S1 TEM images showing the morphology of UiO NMOFs.

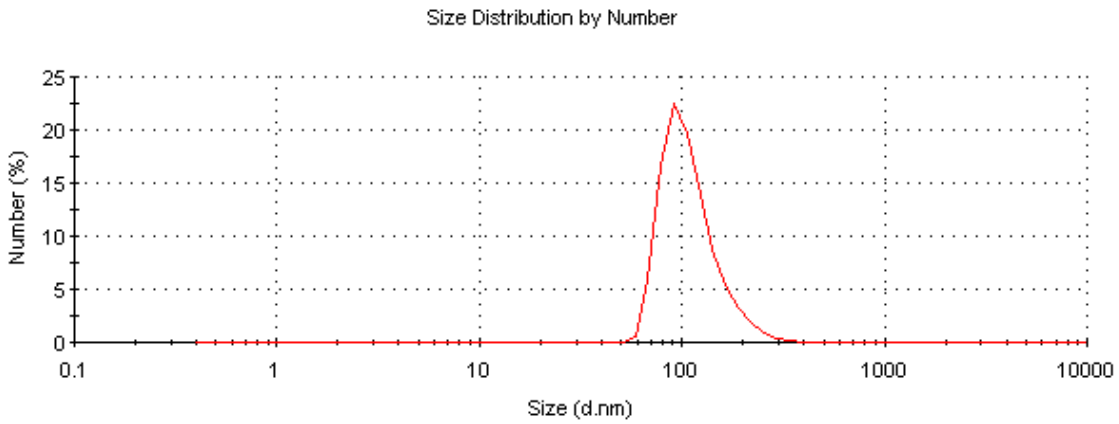

Figure S2 DLS measurement showing the particle size of UiO.

3. Post-synthetic loading of fluorescein isothiocyanate (FITC)

An anhydrous DMF solution of FITC (50 μg/mL) was added to 0.5 mg of UiO NMOF suspended in 0.5 mL of anhydrous DMF. Different FITC feed amounts (from 1 wt.% to 30 wt.%) were used to evaluate the correlation between FITC loading and fluorescence efficiency. The mixture was stirred at room temperature in the dark for 24 hours to afford FITC-conjugated UiO NMOF (F-UiO). The product was collected by centrifugation and washed with DMF, yielding F-UiO with orange color. The supernatants from the washings were quantified by UV-Vis absorption spectroscopy to determine FITC loadings (by subtraction).

The conjugation of FITC to the ligand (amino-TPDC) of UiO was confirmed by ^{1}H NMR spectra (Bruker AVANCE II+ 500; 11.7 Tesla NMR) and mass spectrometry (Agilent 1100 LC/MSD with ESI and APCI ion sources). For NMR analysis, F-UiO was digested in potassium phosphate aqueous solution (deuterated) and DMSO-d_6. The NMR spectra of FITC, F-UiO digest, and UiO digest were obtained in D_2O/DMSO-d_6. For mass spectrometric analysis, F-UiO was digested in potassium phosphate aqueous solution and the ligand was extracted with DMSO. The sample was delivered with methanol. Amino-TPDC (exact mass=333) and FITC-conjugated ligand (FITC-TPDC, exact mass=722) were observed.

Authentic FITC-conjugated amino-TPDC was synthesized and its NMR spectrum was obtained as a comparison to the F-UiO digest. A mixture of amino-TPDC (10.2 mg, 0.031 mmol) and FITC (11.8 mg, 0.030 mmol) was dissolved in 3 mL of anhydrous dimethylsulfoxide (DMSO) in a 20 mL glass vial. The solution was stirred at room temperature in the dark for 6 hours. The solution was lyophilized to remove most of the solvent. The remaining solution (about 0.5 mL) was added to 100 mL of dichloromethane. Yellow precipitate was collected by centrifugation and was washed with dichloromethane. Yield: 62%. ^{1}H-NMR (DMSO-d6): δ=13.01 (br, 2H), 10.13 (s,

2H), 10.02 (s, 1H), 9.86 (s, 1H), 8.06 (d, 2H), 8.05-8.00 (m, 3H), 7.89 (d, 2H), 7.81 (dd, 2H), 7.63 (m, 3H), 7.57 (d, 1H), 7.12 (d, 1H), 6.66 (d, 2H), 6.57 (m, 4H).

The morphology of F-UiO was evaluated by TEM (Figure S5) and the particle size was determined by DLS (Figure S6) and powder X-ray diffraction patterns of UiO NMOF before and after FITC loading were collected on a Bruker D8 Venture, dual microsource (Cu and Mo) diffractometer with a CMOS detector. Cu Kα radiation was used. The PXRD patterns were processed with the APEX 2 package using PILOT plug-in.

(a)

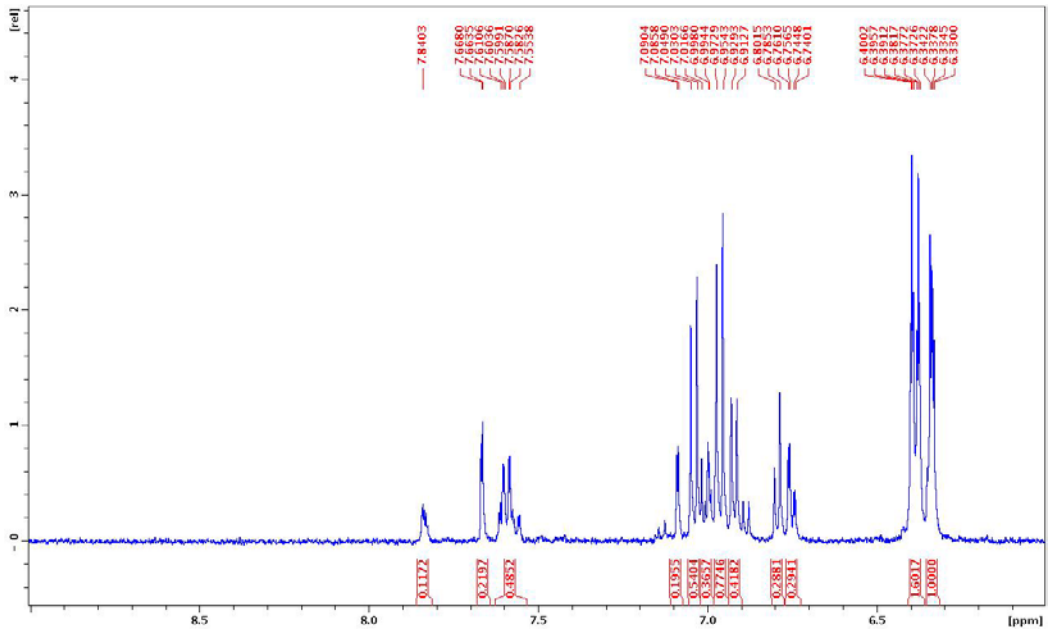

(b)

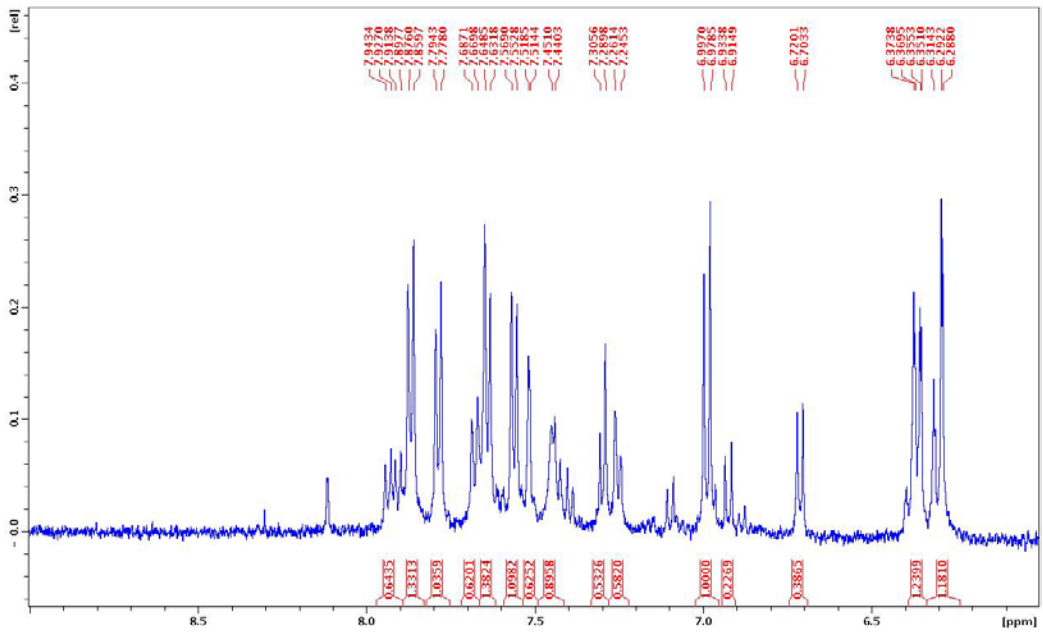

(c)

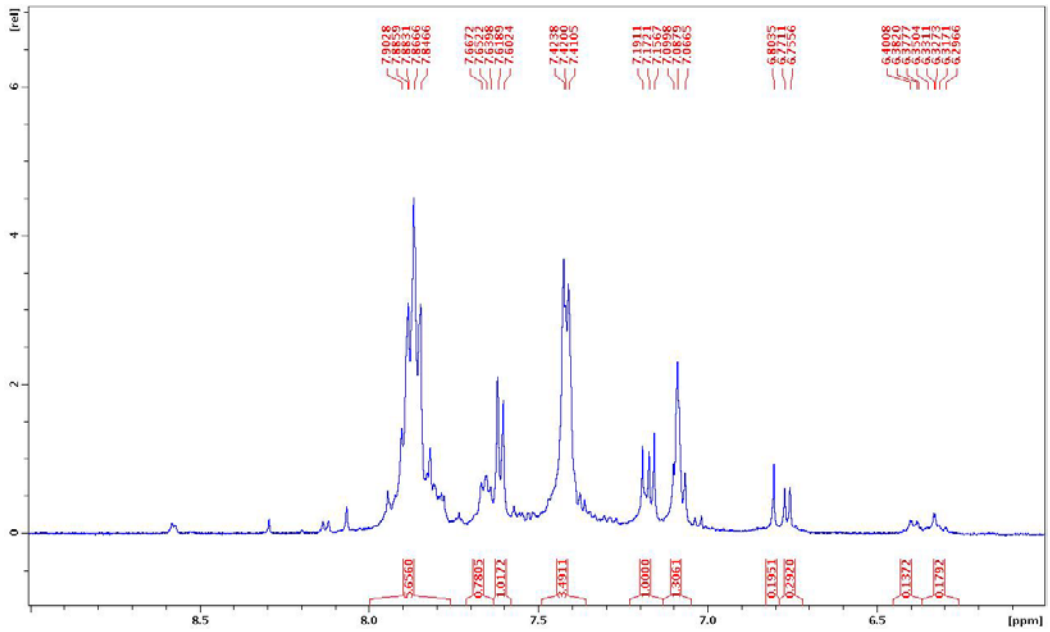

(d)

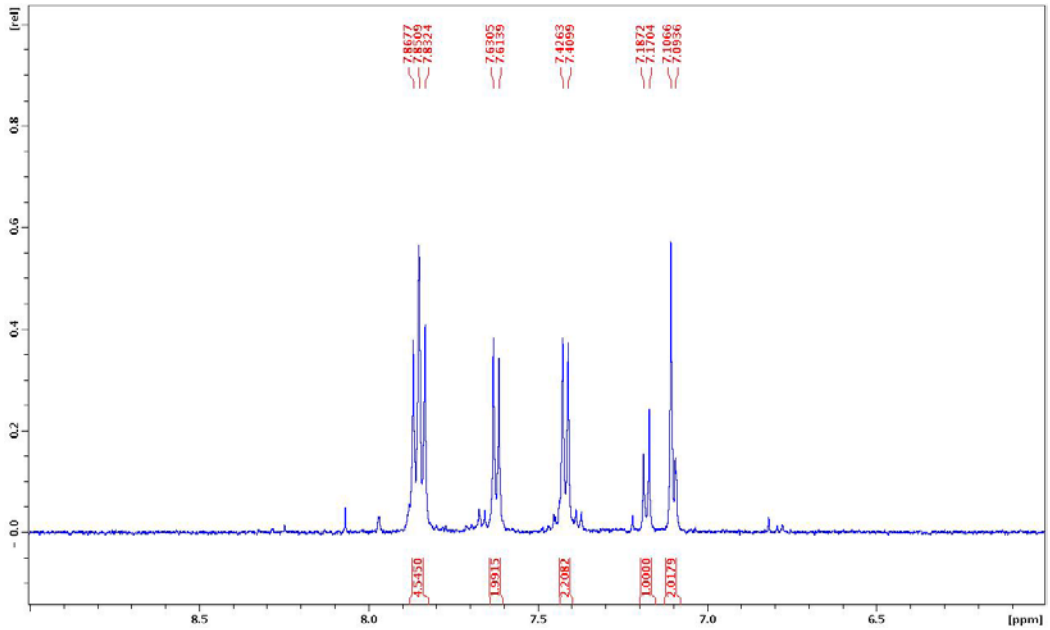

Figure S3 ^{1}H NMR spectra of FITC (a), FITC-TPDC (b), F-UiO digest (c) and UiO digest (d) in D_2O/DMSO-d_6.

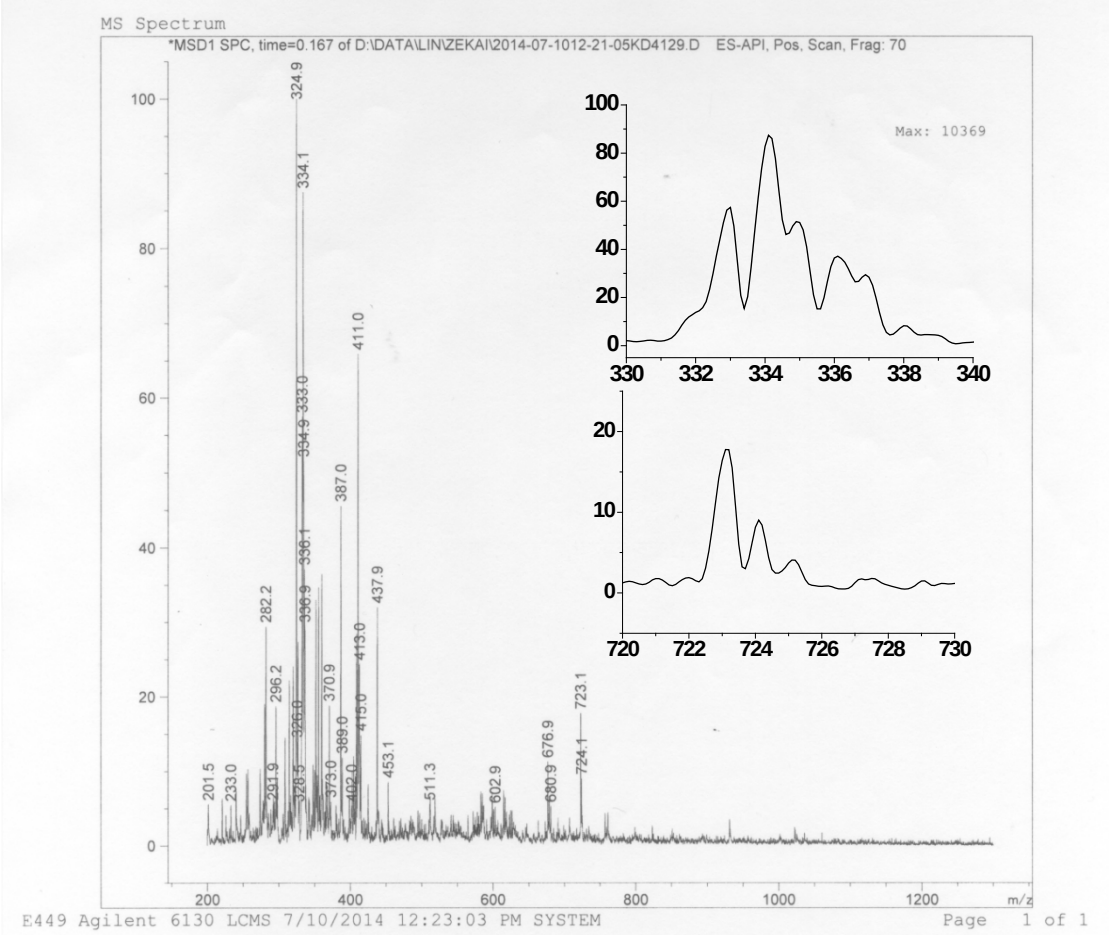

Figure S4 Mass spectrum of F-UiO digest. F-UiO was digested in potassium phosphate aqueous solution and the ligand was extracted with DMSO. The sample was delivered with methanol. Amino-TPDC ligand (exact mass=333) and FITC attached ligand (FITC-TPDC, exact mass=722) were observed.

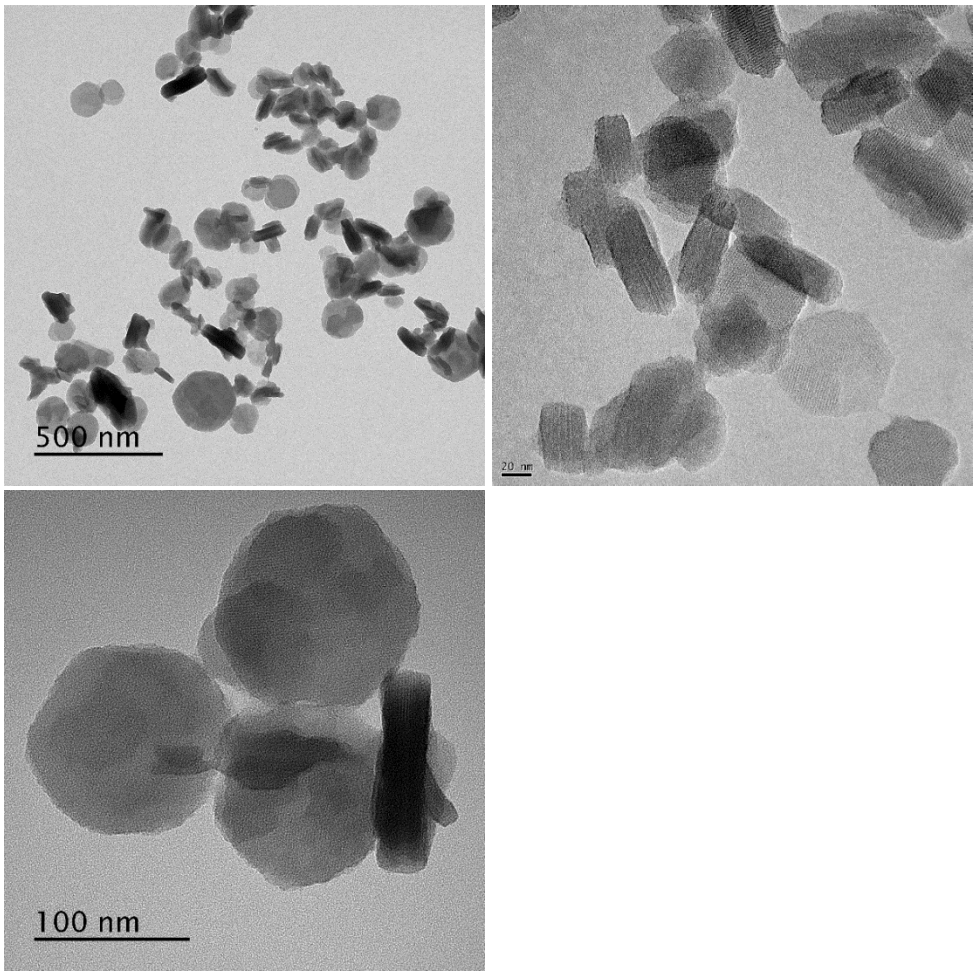

Figure S5 TEM images showing the morphology of F-UiO NMOFs.

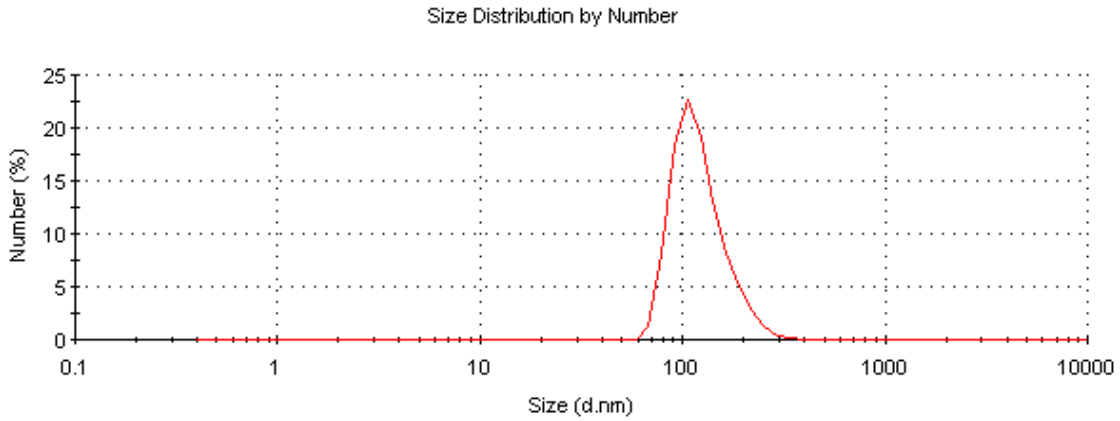

Figure S6 DLS measurement showing the particle size of F-UiO.

4. FITC release

F-UiO (9.5 wt.% FITC loading, 0.22 mg) was washed with water and suspended in 1 mL of Hank's Balanced Salt Solutio (HBSS) buffer by sonication. After incubating for 15 min, 30 min, 1 h, 2 h and 24 h, the suspension was centrifuged at 13,000 rpm for 15 min. Five hundred microliter of the supernatant was collected and another 500 µL of fresh HBSS was added followed by the resuspension of F-UiO. The supernatants were diluted by 5 fold with HBSS and subjected to UV-vis analysis. Accumulative FITC release was calculated by comparing the FITC amount in the supernatant with the total FITC loading.

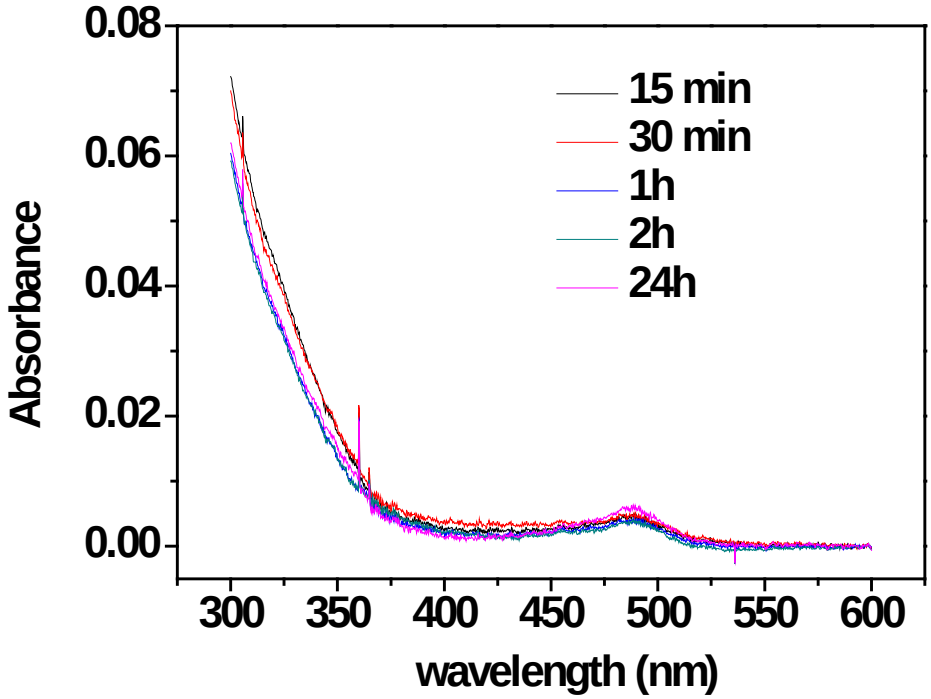

Figure S7 F-UiO was incubated with HBSS for 15 min, 30 min, 1 h, 2 h, and 24 h, respectively. At each time point, F-UiO was centrifuged and the UV-vis spectra of the supernatant was taken.

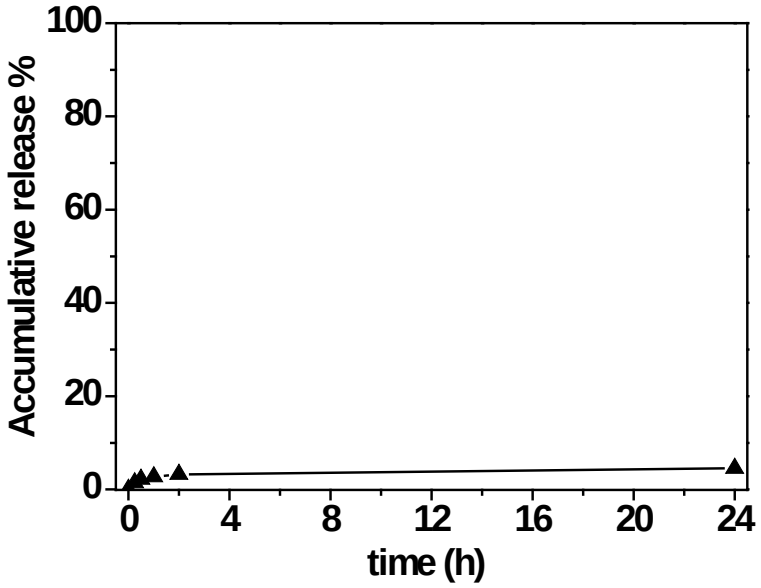

Figure S8 Accumulative FITC release from F-UiO incubated with HBSS over 24 hours. The very small amount of FITC detected in the supernatant could have come from ultrasmall F-UiO particles that could not be centrifuged at 13,000 rpm. Negligible FITC release from F-UiO thus supports its successful conjugation to the amino-TPDC ligand.

5. Structural stability of F-UiO in Hank's Balanced Salt Solution (HBSS)

F-UiO was incubated in HBSS at room temperature for 10 min, 20 min, 30 min, 1 h, 2 h, 12 h, 24 h, and 48 h, respectively. The morphology of HBSS-treated F-UiO was observed by TEM. The PXRD pattern of F-UiO after incubating with HBSS for 12 h was collected and compared to that of F-UiO before HBSS treatment.

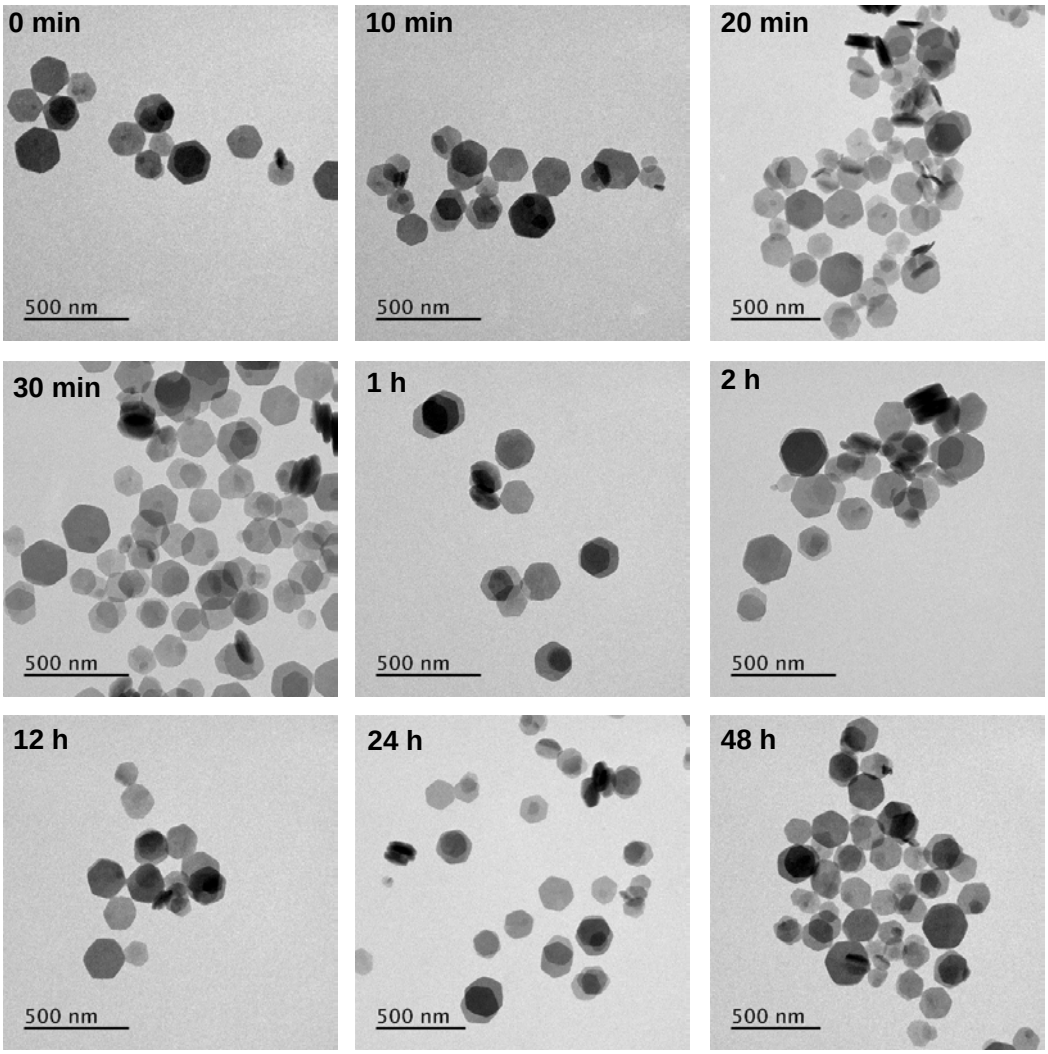

Figure S9 TEM images of F-UiO before and after incubating with HBSS for 10 min, 20 min, 30 min, 1 h, 2 h, 12 h, 24 h, and 48 h.

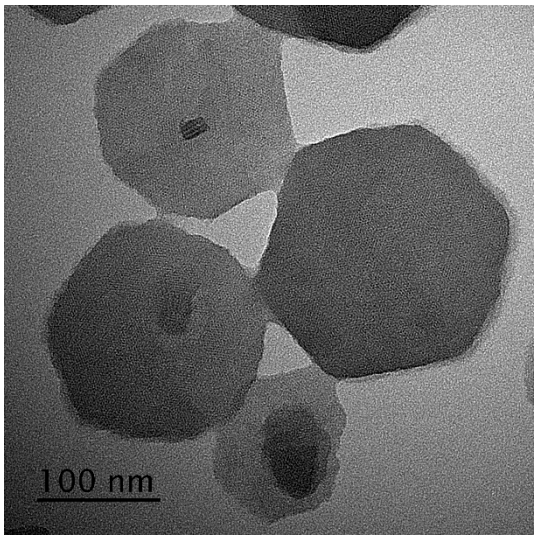

Figure S10 High resolution TEM image of F-UiO incubating with HBSS for 48 h.

6. Quantification of FITC loadings

FITC was dissolved in a triethylamine/DMF (1:9, v/v) solution to obtain a series of FITC solutions with concentrations ranging from 1 to 5 mg/L. Absorption spectra were recorded with a UV-vis spectrophotometer (UV-2401PC, Shimadzu, Japan). A standard curve was plotted from linear fitting of the absorbance at 523 nm as a function of FITC concentrations. The extinction coefficient was determined to be 0.0840 $L \cdot mg^{-1} \cdot cm^{-1}$.

The supernatant collected from each washing step after FITC loading was prepared into 3.3 mL of triethylamine/DMF (1:9, v/v) solution, and the FITC amount was quantified by UV-vis spectrophotometer. The FITC loading amount was calculated by subtracting the amount in the supernatant (unloaded) from the feed amount.

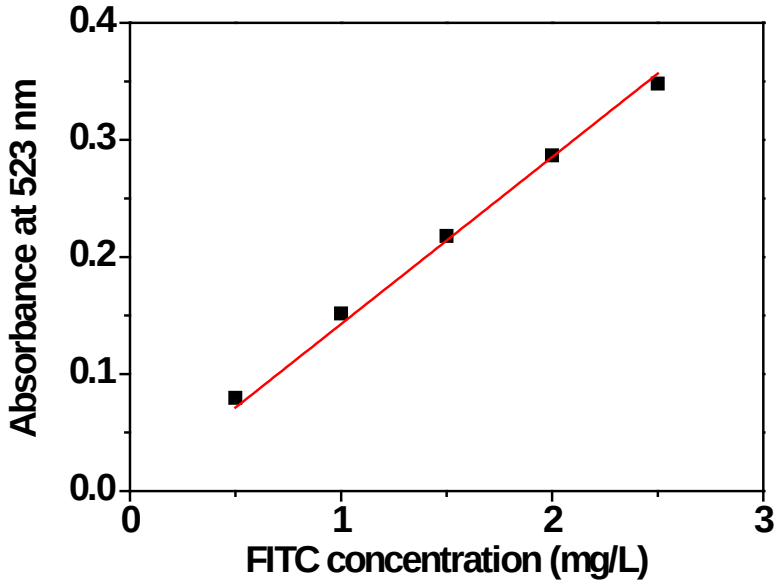

Figure S11 Standard curve of FITC in triethylamine/DMF (1:9, v/v) solution by UV-vis.

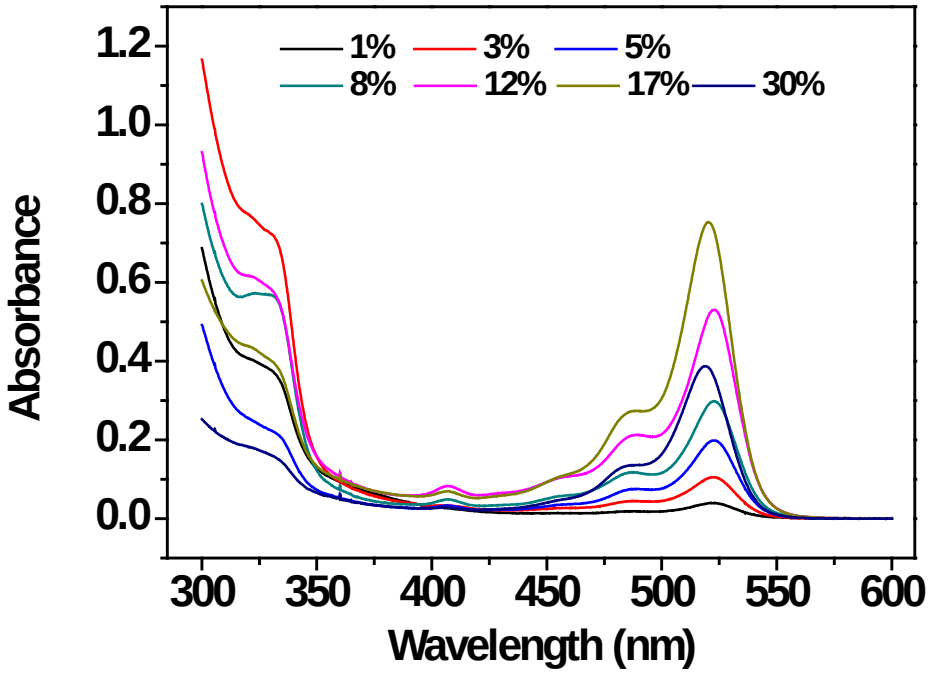

Figure S12 Absorbance spectra of the supernatant collected from each washing step after FITC loading at a series of FITC feed amount percent. Numbers shown in the figure legend represent the FITC feed wt.%. The supernatant collected from FITC loading at a FITC feed of 17 wt.% and 30 wt.% was diluted with triethylamine/DMF (1:9, v/v) solution before determination.

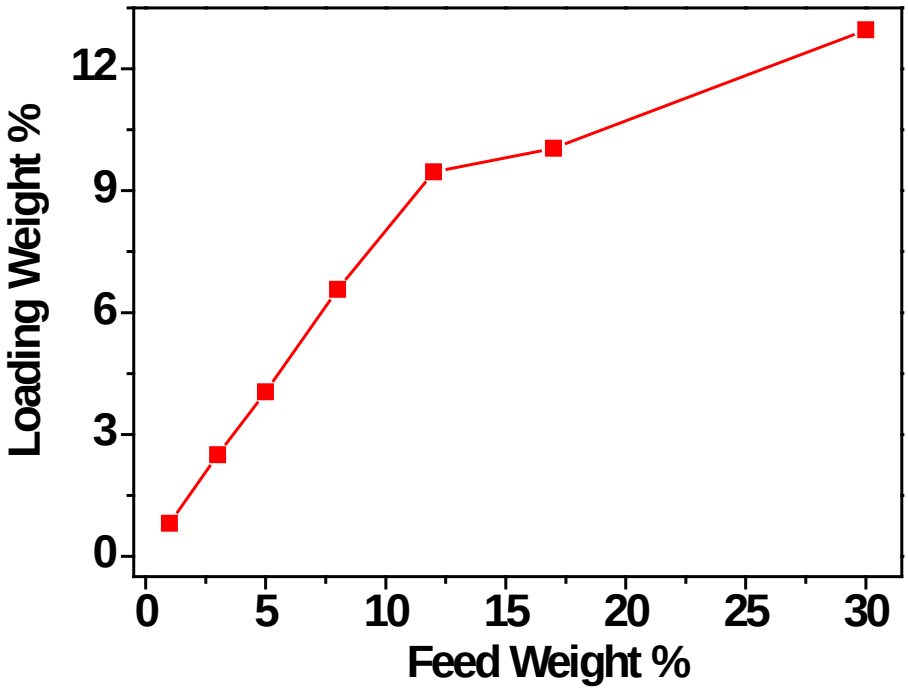

Figure S13 Correlation between FITC feed weight% and FITC loading weight%.

7. Fluorescence efficiency of F-UiO with different FITC loadings

UiO and F-UiO NMOFs with different dye loadings were dispersed in phosphate buffered solution (PBS) at an NMOF concentration of 50 mg/L. The absorption spectra of F-UiO were acquired and corrected by eliminating the scattering background from blank UiO NMOFs. Meanwhile, the fluorescence intensity of F-UiO was determined at excitation wavelength of 490 nm and emission wavelength of 516 nm. The absorbance at 490 nm and fluorescence intensity of F-UiO (excitation at 490 nm and emission at 516 nm) were plotted against FITC loading amount. A saturation of fluorescence was observed at FITC loading amount higher than 7%. However, no saturation was noticed for absorbance of F-UiO at FITC loading amount up to 13%.

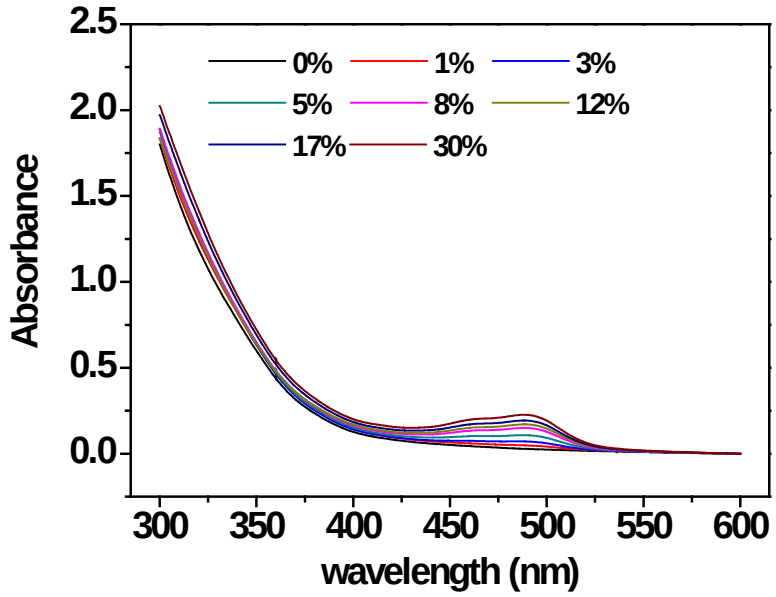

Figure S14 Absorption spectra of blank UiO NMOFs and F-UiO NMOFs at a series of FITC loading amounts. Numbers shown in the figure legend represent the FITC feed wt.%.

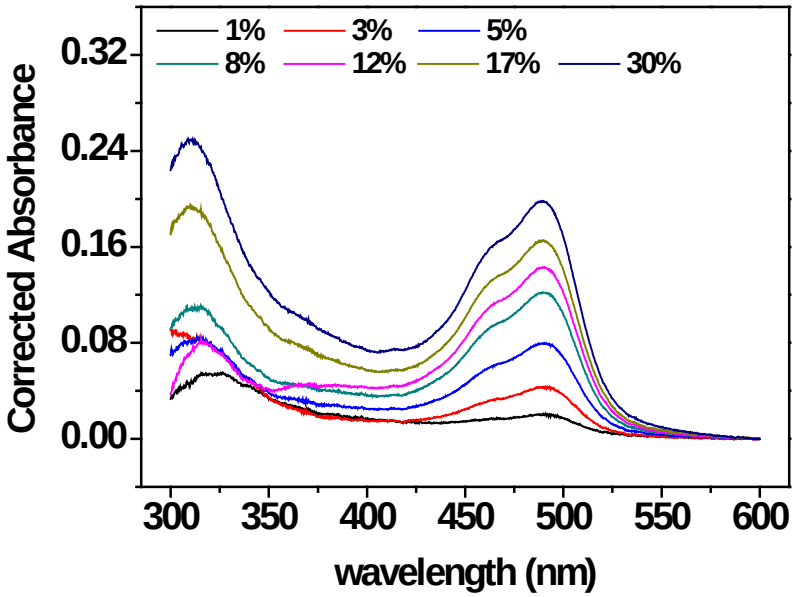

Figure S15 Absorption spectra of F-UiO NMOFs at a series of FITC loading amounts after background correction (from particle scattering). Numbers shown in the figure legend represent the FITC feed wt.%.

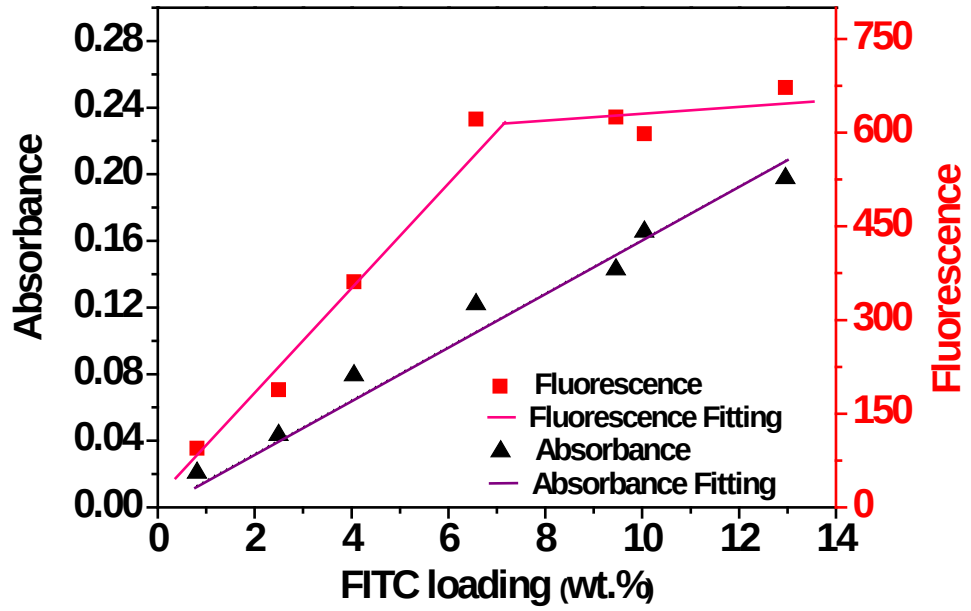

Figure S16 Fluorescence efficiency of F-UiO with different FITC loadings. The absorbance was acquired at 490 nm and the fluorescence intensity was detected at excitation/emission wavelength of 490 nm/516 nm.

8. Ratiometric pH calibration and measurements in buffers

The pH response of F-UiO was evaluated in buffered solution with pH ranging from 4.0 to 8.0 with a spectrofluorophotometer (RF-5301PC, Shimadzu, Japan) and by confocal laser scanning microscopy (CLSM, Leica SP5 II, Integrated Microscopy Core Facility at the University of Chicago).

For the calibration by fluorimetry, 20 μL of 1 mg/mL F-UiO or 0.1 mg/mL FITC free solution was added to 2 mL of buffered solution (acetic buffered solution for pH 4.0-6.0 and phosphate buffered solution for pH 6.5-8.0), respectively. Fluorescence spectra were recorded using two excitation wavelengths, 435 nm and 488 nm. The fluorescence emission intensity ratio was calculated at emission wavelength of 520 nm. An pH calibration curve was obtained by plotting the ratio of fluorescence intensity at 488 nm and 435 nm ($I_{488/520}$:$I_{435/520}$) as a function of pH.

For the calibration by CLSM, 1 μL of 1 mg/mL F-UiO was mixed with 9 μL of HBSS Hank's Balanced Salt Solution of which the pH was adjusted by 1 M NaOH or 1 M HCl to 4.0-8.0, and added to a glass-bottom petri dish (No. 1.5, uncoated glass, MatTek Corporation). The images were acquired using two different lasers (435 nm and 488 nm) and the same filter for 488 nm laser by CLSM. The fluorescence intensity of

NMOF particles at dual excitation wavelengths was quantified directly from the images using Image J, and the fluorescence emission intensity ratio (488 nm versus 435 nm) was calculated accordingly. An in vitro pH calibration curve was obtained by plotting the ratio of fluorescence intensity at 488 nm and 435 nm ($I_{488/520}$:$I_{435/520}$) as a function of pH.

The fluorescence emission intensity ratio to pH plot was similar to titration curve, indicating that the pH response likely result from a deprotonation process. The pKa of fluorescein mono-anion is 6.7. The di-anion form of fluorescein has higher absorbance at 490 nm than its mono-anion form while the 435 nm absorption peak disappears.[2,3] In order to better understand and analyze the correlation between fluorescence emission intensity ratio and pH, a fitting was performed as follows:

HA and A were used herein to refer to mono- and di-anionic forms of FITC, respectively. Since the former proton dissociation doesn't contribute to the ratiometric change of FITC fluorescence,[3] the former steps of proton dissociation were ignored. The concentration of each species is:

$$[HA] = c_0 \frac{[H^+]}{[H^+]+K}$$

$$[A] = c_0 \frac{K}{[H^+]+K}$$

where c_0 is the total concentration of FITC, and K is the dissociation constant of the aforementioned step.

The fluorescence intensity is linearly correlated to FITC specie concentrations:

$$I_f = I_0 \phi_f \varepsilon b c = kc$$

$$I_{488nm} = k_{a1}[HA] + k_{b1}[A]$$

$$I_{435nm} = k_{a2}[HA] + k_{b2}[A]$$

where I_0, ϕ_f, ε, b, and c are incident light intensity, quantum yield, extinguish coefficient, path length, and the concentration of the solution, respectively.

The fluorescence emission intensity ratio is:

$$r = \frac{I_{488nm}}{I_{435nm}} = \frac{k_{a1}[H^+]+k_{b1}K}{k_{a2}[H^+]+k_{b2}K} = \frac{\frac{k_{a1}}{k_{a2}}[H^+]+\frac{k_{b1}}{k_{a2}}K}{[H^+]+\frac{k_{b2}}{k_{a2}}K}$$

$$r = \frac{\frac{k_{a1}}{k_{a2}}e^{-2.303\,pH}+\frac{k_{b1}}{k_{a2}}K}{e^{-2.303\,pH}+\frac{k_{b2}}{k_{a2}}K}$$

Therefore, the fluorescence emission intensity ratio against proton activity fits a non-linear regression in a form of:

$$y = \frac{P_1 x + P_2}{x + Q_1}$$

where

$$P_1 = \frac{k_{a1}}{k_{a2}}$$

$$P_2 = \frac{k_{b1}}{k_{a2}} K$$

$$Q_1 = \frac{k_{b2}}{k_{a2}} K$$

Based on this hypothesis, we ran the regression on MatLab, which gave the following results:

(1) For free FITC solution by fluorimetry:

$$r = \frac{0.98[H^+] + 7.42 \times 10^{-6}}{[H^+] + 4.74 \times 10^{-7}}$$

adjusted r^2=0.99

(2) For F-UiO by fluorimetry:

$$r = \frac{1.05[H^+] + 8.17 \times 10^{-6}}{[H^+] + 6.14 \times 10^{-7}}$$

adjusted r^2=0.99

(3) For F-UiO by CLSM:

$$r = \frac{1.11[H^+] + 8.61 \times 10^{-6}}{[H^+] + 6.24 \times 10^{-7}}$$

adjusted r^2=0.99

Additionally, the errors of pH were calculated from the errors of fluorescence emission intensity ratios were based on these equations:

$$[H^+] = Q_1 \left(\frac{H - L}{r - L} - 1 \right)$$

$$\frac{dpH}{dr} = \frac{\frac{1}{2.303}(H - L)}{(r - L)(H - r)}$$

where H and L are upper limit and lower limit of *r*, respectively,

$$H = \frac{P_2}{Q_1}$$

$$L = P_1$$

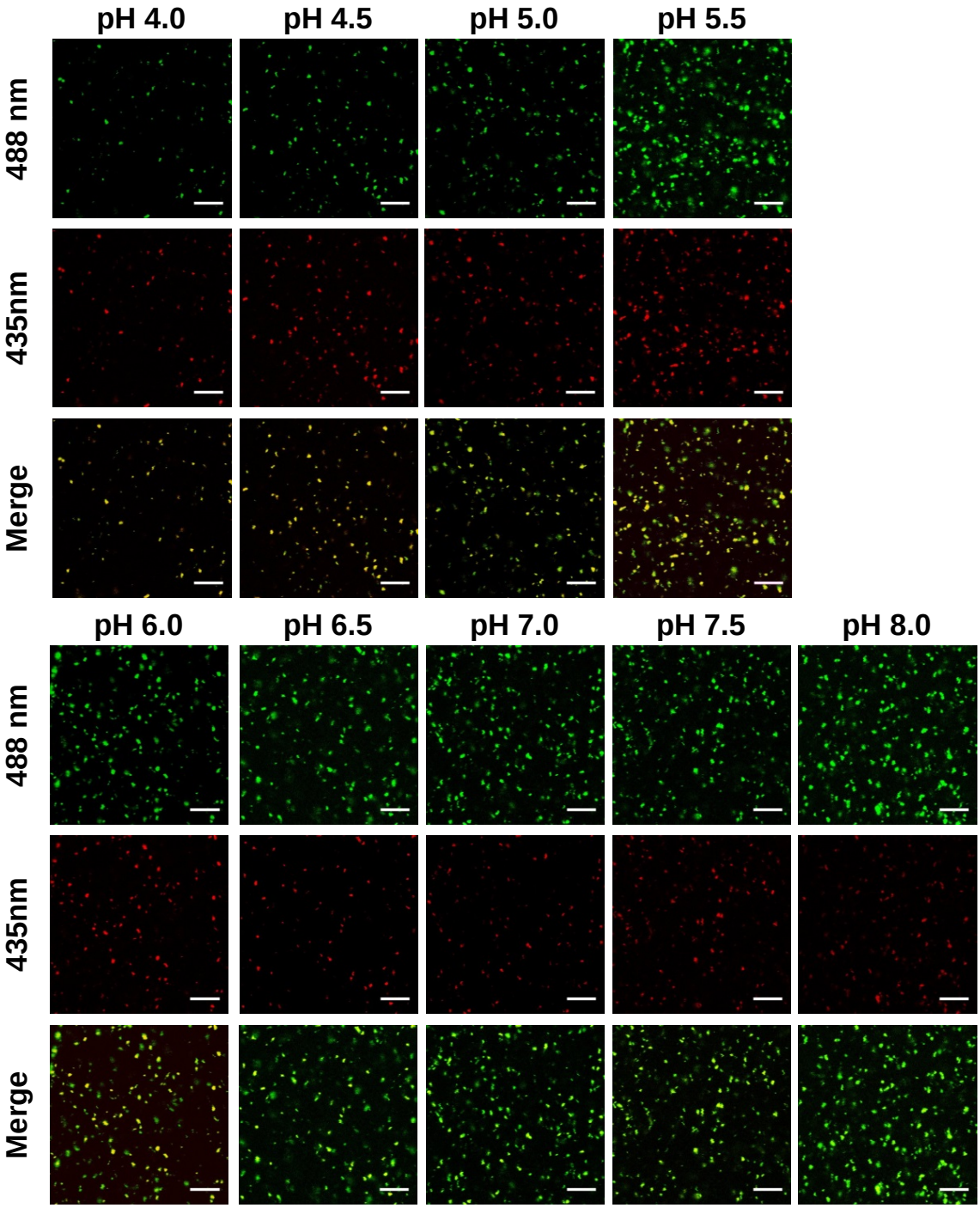

Figure S17 Images of F-UiO dispersed in HBSS with a series of pH acquired by CLSM using dual excitation at wavelengths of 488 nm and 435 nm, respectively, and the same emission wavelength of 520 nm. Bar represented 5 μm.

9. Ratiometric pH calibration and measurements in live cells

pH clamping and measurement experiments were performed on live cells. H460 cells were seeded on a glass-bottom petri dish (No. 1.5, coated with poly-lysine, MatTek Corporation) at cell density of 5×10^5 cells and further cultured for 24 h. The cell culture medium was removed and replaced with fresh HBSS. The cells were further cultured with F-UiO for 2 h. After the incubation, the HBSS was removed and replaced by clamping buffers (120 mM KCl, 5 mM NaCl, 1 mM $MgCl_2$, 1 mM $CaCl_2$, 20 mM HEPES) of pH ranging from 4.0 to 8.0, containing 100 μM nigericin.

Images were collected using Leica SP5 II microscope equipped with 100X, 1.4 oil objective, PMT fluorescence detector, transmitted light detector with DIC polarizer, and full wrap incubator box with warm air heating for live samples controlled by LAS_AF Leica confocal software. For pH measurements, cells were imaged in three channels to yield three images, (i) exciting at 488 nm and collecting at 520 nm (ii) exciting at 435 nm and collecting at 520 nm (iii) DIC. Mean intensity of F-UiO inside the cells was measured in 488 nm and 435 nm channels and a ratio of 488 nm to 435 nm intensities of F-UiO was obtained. The pH was plot against $I_{488/520} : I_{435/520}$.

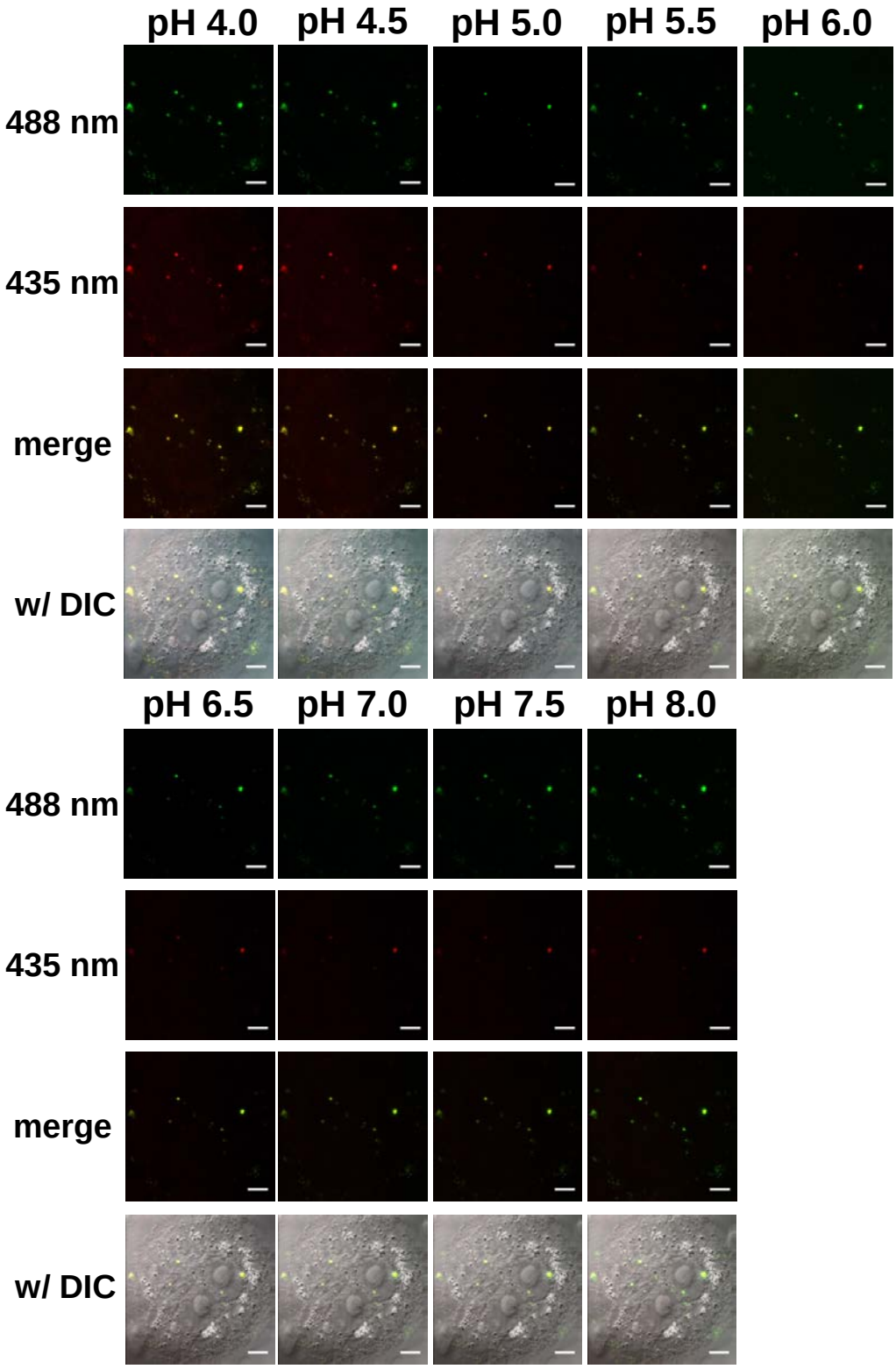

Figure S18 CLSM images of live cells clamped at various pH. Bar = 5 μm.

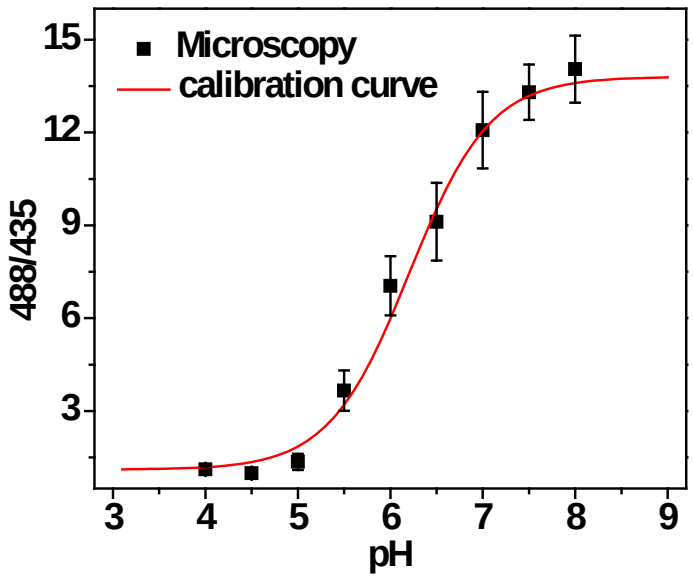

Figure S19 pH calibration in live cells by clamping the cells at various pH values. The cells were imaged by CLSM and analyzed by Image J. The pH was plot against $I_{488/520}$:$I_{435/520}$ (488/435) and compared to the pH calibration curve of F-UiO obtained by CLSM.

10. Cellular uptake in H460 cells

10.1. Time-dependent cellular uptake

H460 cells were seeded on a 6-well plate at 1×10^6 cells per well and cultured for 24 h. Thirty microliter of 2 mg/mL F-UiO were added to each well. After a 10-min, 20-min, 30-min, and 120-min incubation, cells were collected by cell scraper, washed with PBS three times, and counted with hemocytometer. The cells were centrifuged at 3,000 rpm for 5 min and the cell pellet was digested with 500 μL of concentrated nitric acid. After 24 h, the digestion was diluted with water and subjected to inductively coupled plasma mass spectrometry (ICP-MS, Agilent 7700X) to determine the Zr concentration. Results were expressed as the amount of F-UiO (pg) calculated from the Zr concentration associated with one cell.

10.2. TEM observation

The uptake and intracellular trafficking of UiO NMOFs in H460 cells were directly observed by TEM. H460 cells were seeded on 10-cm petri dish at 2×10^6 cells and cultured for 24 h. Two hundred microliters of 1 mg/mL UiO NMOFs were added to the cells. Following incubating for 2 h, the cells were fixed, sectioned at 40-70 nm thickness, and observed under TEM.

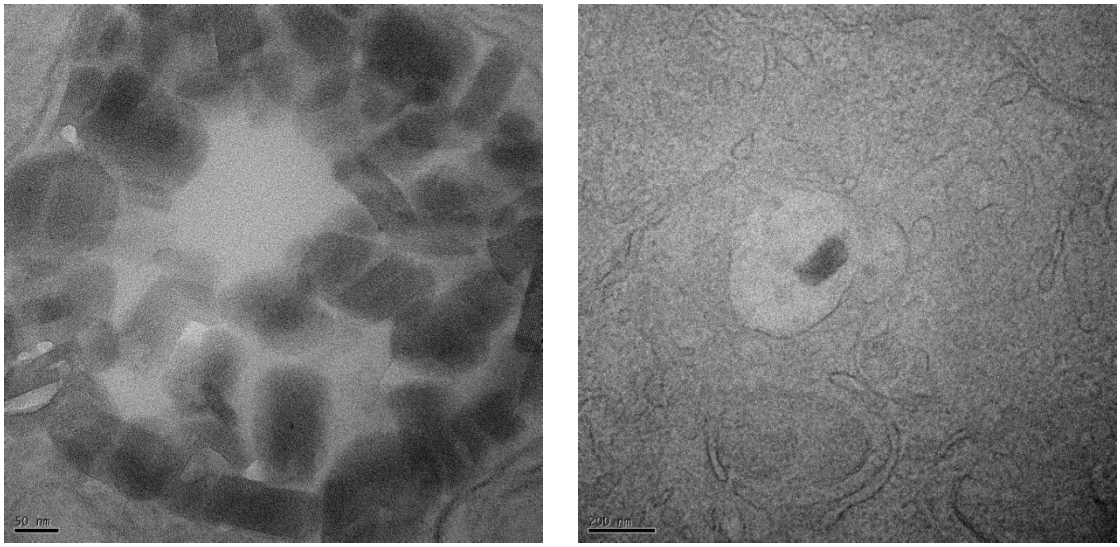

Figure S20 High-resolution TEM images revealing the structural integrity of UiO NMOFs entrapped in one single endosome.

11. Live cell image acquisition and analysis

H460 cells were seeded on a glass-bottom petri dish (No. 1.5, coated with poly-lysine, MatTek Corporation) at cell density of 5×10^5 cells and further cultured for 24 h. The cell culture medium was removed and replaced with fresh HBSS before live cell imaging to avoid autofluorescence coming from the culture medium. The live cell imaging started right after adding 25 µL of 1 mg/mL F-UiO to the cells. Images were collected using Leica SP5 II microscope equipped with 100X, 1.4 oil objective, PMT fluorescence detector, transmitted light detector with DIC polarizer, and full wrap incubator box with warm air heating for live samples controlled by LAS_AF Leica confocal software. For pH measurements, cells were imaged in three channels to yield three images, (i) exciting at 488 nm and collecting at 520 nm (ii) exciting at 435 nm and collecting at 520 nm (iii) DIC. Cross talk and bleed-through were measured and found to be negligible for the present experimental setup. No autofluorescence was observed on blank cells. A time relapse experiment was carried out to monitor the endocytosis and exocytosis of F-UiO in H460 cells at a time interval of 20 s and a total time ranging from 15 to 18 minutes. Z-stack scanning was applied to each frame. Mean intensity of F-UiO was measured in 488 nm and 435 nm channels and a ratio of 488 nm to 435 nm intensities of F-UiO was obtained. The pH evolution of F-UiO experienced was calculated from the pH calibration curve obtained before.

Orthogonal views of the cells showing in video 1 were generated to confirm the F-UiO of which the pH did not change overtime was stuck on the cell membrane.

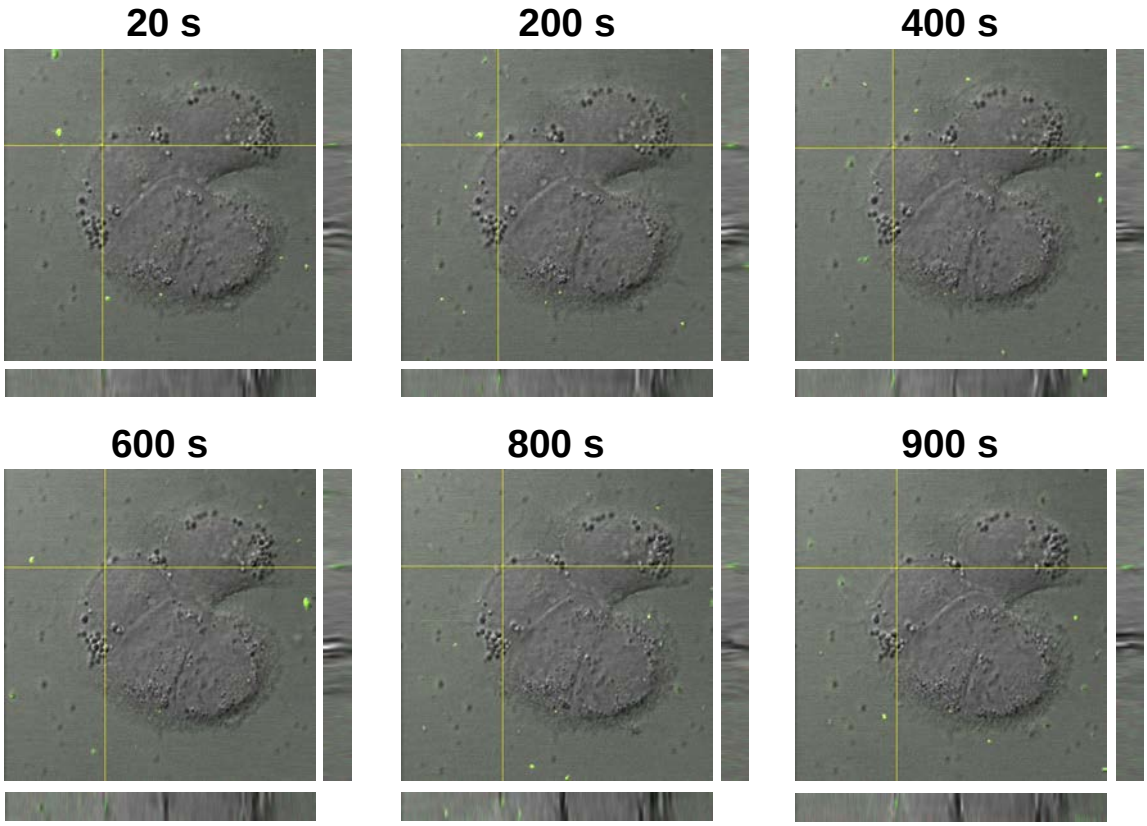

Figure S21 Orthogonal views of cells incubated with F-UiO showing that the particle of interest was stuck on the cell membrane over time. Images were obtained from video 1 and showed the overlay of green fluorescence (488 nm channel), red fluorescence (435 nm channel), and DIC.

12. Intracellular pH sensing in fixed cells

H460 cells were seeded on a glass-bottom petri dish (No. 1.5, coated with poly-lysine, MatTek Corporation) at cell density of 5×10^5 cells and further cultured for 24 h. The cell culture medium was removed and replaced with fresh HBSS. The cells were incubated with F-UiO for 5 min, 10 min, and 20 min, and fixed with 4% paraformaldehyde. The cells were imaged using Leica SP5 II microscope equipped with 100X, 1.4 oil objective, PMT fluorescence detector, and transmitted light detector with DIC polarizer. For pH measurements, cells were imaged in three channels to yield three images, (i) exciting at 488 nm and collecting at 520 nm (ii) exciting at 435 nm and collecting at 520 nm (iii) DIC. Mean intensity of F-UiO was measured in 488 nm and 435 nm channels and a ratio of 488 nm to 435 nm intensities of F-UiO were obtained. pH was calculated from the pH calibration curve obtained before.

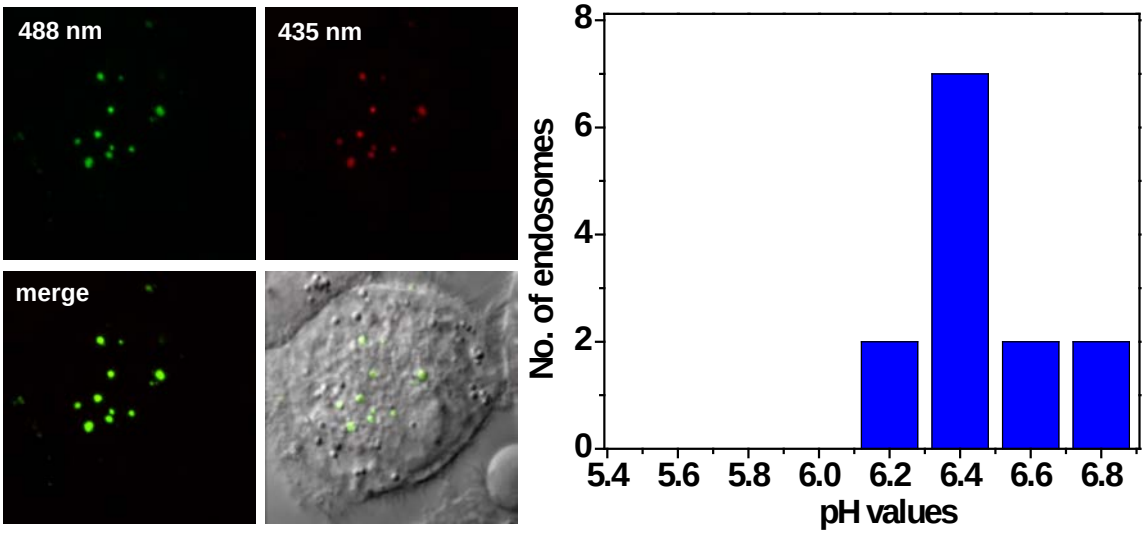

Figure S22 H460 cells were incubated with F-UiO with 5 min and imaged with CLSM after fixation. The histogram shows the number of endosomes at different pH's.

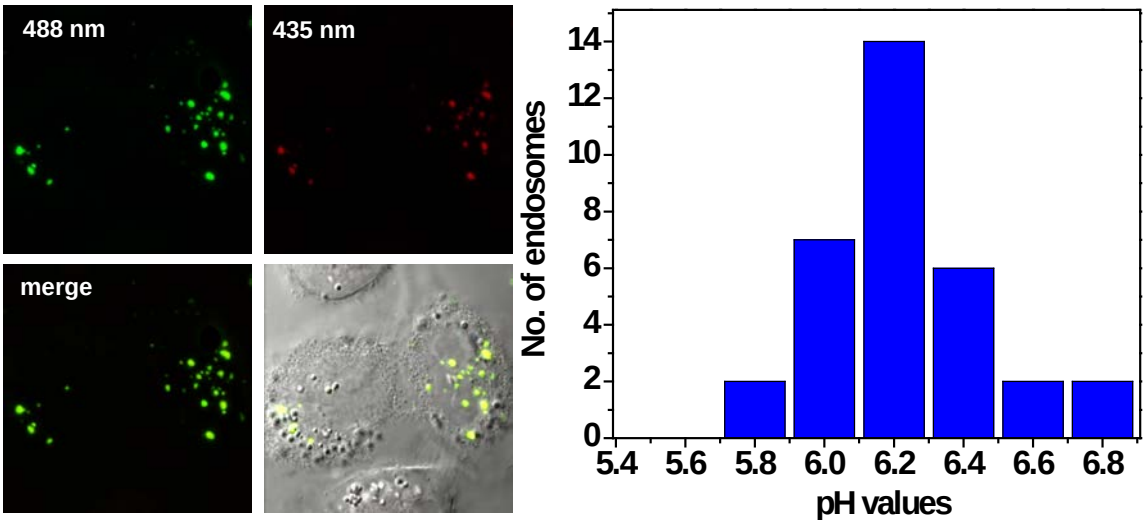

Figure S23 H460 cells were incubated with F-UiO with 10 min and imaged with CLSM after fixation. The histogram shows the number of endosomes at different pH's.

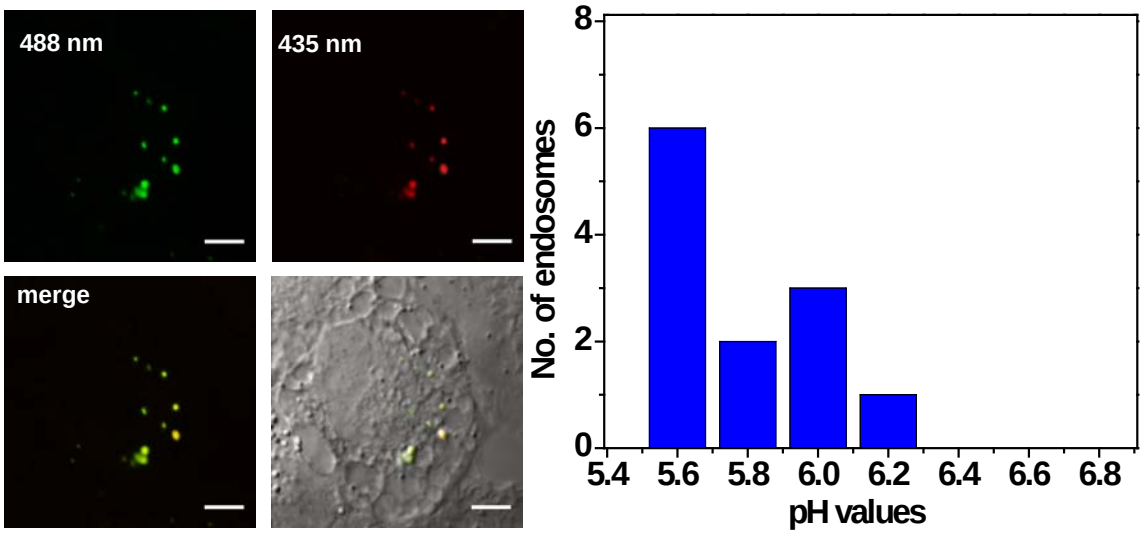

Figure S24 H460 cells were incubated with F-UiO with 20 min and imaged with CLSM after fixation. The histogram shows the number of endosomes at different pH's.

13. References

(1) He, C. B.; Lu, K. D.; Liu, D. M.; Lin, W. B. *J Am Chem Soc* **2014**, *136*, 5181.
(2) Alvarez-Pez, J. M.; Ballesteros, L.; Talavera, E.; Yguerabide, J. *J Phys Chem A* **2001**, *105*, 6320.
(3) Martin, M. M.; Lindqvist, L. *J Lumin* **1975**, *10*, 381.